Frontiers in Heat and Mass Transfer (FHMT), 18, 30 (2022)
DOI: 10.5098/hmt.18.30

Global Digital Central
ISSN: 2151-8629

Frontiers in Heat and Mass Transfer

Available at www.ThermalFluidsCentral.org

NUMERICAL SIMULATION OF MIXED CONVECTIVE FLOW OVER TRIANGULARLY ARRANGED CYLINDERS

O. M. Oyewola[a,b,*], O. S. Ismail[b], M. O. Olasinde[b] , O. O. Ajide[b]

[a] *School of Mechanical Engineering, Fiji National University, Suva, Fiji*
[b] *Department of Mechanical Engineering, University of Ibadan, Ibadan, Nigeria*

ABSTRACT

In this work, attempt is made to investigate the effect of cylindrical arrangement on the thermal and flow fields within the mixed convective regime for different values of Reynolds number within the study zone. Constructal design was used to design the flow geometric. Two-dimensional unsteady laminar flow equations with buoyancy force were solved numerically using finite element technique implemented on ANSYS FLUENT software. The study showed an optimised arrangement of 50% difference in coefficient of drag and 10% difference in Nusselt number within the geometrical arrangement variation. The effect of geometric arrangement is pronounced at low Ri than at high Ri. The result shows that buoyancy force and inertia force have significant effect on the Nusselt number and drag coefficient, respectively. Evidently, wake formation and vortex shedding variation with flow regimes both at the local and general levels may render the flow classification based on Richardson number objectionable especially with the present flow conditions.

Keywords: Numerical analysis, Richardson number, Flow regime, Geometric arrangement, MANOVA.

1. INTRODUCTION

The study of the behaviour of heat transfer by convection is not easy since time dependent flow fields such as vortex are always present which make generalization impossible. In view of the behaviour of flow base on Reynolds number, Price *et al.* (1995) observed that at low Re, symmetric attached vortices behind the cylinder occurred at a critical Re, the dividing line between these symmetry vortices becomes unstable and folds up on itself, resulting in alternate vortex shedding, while for other rigid arrangement no vortex shedding was observed but attached eddies of recirculation flow did form behind the cylinder. This leads to variation of coefficient of drag. Also, if heat is to be transferred, Nusselt number would vary. Vortex formation at different Reynolds number effect on heat transfer and fluid flow was conducted by Alinejad (2016) where lattice Boltzmann method was used to simulate heat transfer in the flow past three arrangements of elliptical and circular cylinders under an isothermal boundary condition.

It worth noting that various works using different object geometric such as cylindrical, rectangular, triangular etc have been done in order to achieve certain target (Mejbel *et al.,*2020 and Wang *et al.,* 2021). For instance, one of the early works was done by Zdravkovich (1977) where geometrics such as rectangular, circular, rectangular conduit etc. were used to transfer heat and fluid. Interestingly, out of the geometrics, cylinder have received high research interest due to its relatively ease of construction, low drag and high heat transfer rate (Mohd *et al.,* 2022; Mejbel *et al.,* 2020; Price *et al.,* 1995 and Ohya *et al.*, 1989). This is not surprising since group of cylindrical bodies of different arrangement may be used for efficient heat transfer. Investigation of the flow and thermal characteristics of such arrangement is very important to determine how efficient they are and whether they can be optimized further (Sahu and Singh 2014). Laminar natural convection over heated horizontal cylinders of a triangular cross-section was numerically investigated by Alansar *et al.,* (2012) using FLOWWORKS software. The authors result showed that the heat parameters are function of Rayleigh number. Also, Sahu and Singh (2014) simulated heat transfer and flow due to natural convection in air around heated equilateral triangular cylinders of different sizes inside a square enclosure using CFD package. The authors result showed that heat and flow fields are function of flow regimes. Elaborate investigations of discontinuities of pressure distributions on two circular cylinders in staggered arrangement were given by (Gu and Sun 1999).

The geometric configuration is as good as selection of geometric. Geometric arrangement or configuration requires the process of determining the appropriate coordinate of geometric for optimal heat transfer at a reduced pumping power. Different approaches have been used to determine the optimized coordinate of geometric such as genetic algorithm, neural network, constructal design, statistical tools etc. In term of cylindrical arrangement, three heated cylinders in triangular arrangement in a flow were numerically investigated by (Barros *et al.,* 2017). The authors showed that buoyancy forces in mixed convective flows have strong influence over design of the studied cylinders arrangement and that there is no optimised design for a triangular cylinder within a mixed convective zone. However, variation in Reynolds numbers in order to investigate the behaviour at that condition was not considered. Bello-Ochende and Bejan (2004) also worked on the optimal spacing and the dimensionless groups that governed flow parameters (Rayleigh number, pressure drop number, mixed convection ratio). The authors showed that flow classification based on dimensionless number is not always valid, leading to the modification of convection regimes. Further, Wang (1998) worked on longitudinal flow past cylinders arranged in a triangular array using perturbation method. The author found that regime of flow determines the flow field, nevertheless information about regime changes were not specified.

Vortex formation and shedding are very important phenomenon that affect heat transfer and coefficient of friction in a cross flow. Johansson

* Corresponding author. Email: olanrewaju.oyewola@fnu.ac.fj

Global Digital Central
ISSN: 2151-8629

et al., (1993) analyzed unsteady turbulent flow around and behind triangular-shaped flame holders using a finite volume code with a k—ε model of turbulence. The authors discovered that to capture the vortex street, it is very important that the grid spacing is sufficiently fine. Moreover, Lam and Cheung (1988) studied phenomena of vortex shedding and flow interference of three cylinders in different equilateral arrangements, using dye-injection technique flow visualization. Their results indicated that vortex shedding varied with flow regimes. Further, Hu and Koochesfahani (2005) studied the wake behaviour behind a heated cylinder in forced and mixed convection regimes. The authors showed that with increase in Richardson number, significant modifications of the wake instability were revealed from qualitative flow visualization images for single cylinder in a cross flow. Also, Abo *et al*., (2015) numerically investigated a three dimensional laminar mixed convection flow in lid-driven cavity for very small Richardson number. They found that the average Nusselt number on the top and bottom surfaces decreases for all sections inside the cavity with increase in Richardson number. In addition, they found that heat transfer varied with the dimensionless number.

Despite numerous works on cylinders with various arrangements from experimental and numerical point of views, there are still a lot of unresolved issues. For instance, the response of the thermal and flow fields within the mixed convective regime to the Reynolds number with reference to triangularly arranged cylinder is yet unclear. This is necessary in order to obtain an optimized heat exchanging system. Therefore, this present work numerically simulates convective heat transfer within the region 0.1<Ri<10 for triangularly arranged constant diameter cylinders using the physical model used by Barros *et al.* (2017) with the view of examining the effect of cylindrical arrangement on the thermal and flow fields within the mixed convective regime for various values of Reynolds numbers, while the Grashof number is kept constant. In addition, Analysis of Variance (ANOVA) and MANOVA were used to determine how significant Nusselt number and drag coefficient changes at 5% confidence level. The application of this work is in the optimization of heat exchanging systems by minimizing the energy loss in the form of heat and power as a result of high drag coefficient.

2. PROBLEM DESCRIPTION AND NUMERICAL EQUATIONS

The cylinders are arranged inside the rectangular channel triangularly as used by Barros *et al.* (2017). Air at temperature T∞ and velocity U∞ is blown over heated triangular arranged cylinder at constant surface temperature Ts through a channel. The flow field and thermal field characteristics are to be obtained for each cylinder. The Nusselt numbers and coefficient of drag of the three cylinders are summed and averaged to obtain the representative Nusselt number and coefficient of drag.

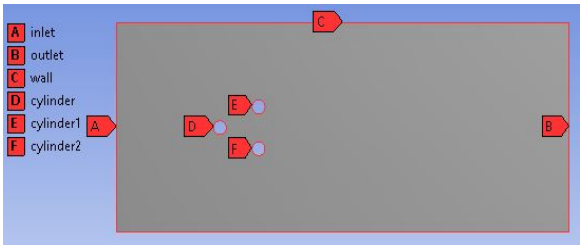

Fig. 1 Schematic diagram of the configuration

Buoyancy effects can significantly enhance heat transfer for laminar forced convection flows, enhancement is typically negligible if the forced flow is turbulent Osborne and Incropera (1985). Hence, the governing equation of flow that is used is an unsteady, two-dimensional laminar flow with supporting buoyancy force taking into consideration. The equations in its general form are:

$$\frac{\partial u}{\partial x}+\frac{\partial v}{\partial y}=0 \tag{1}$$

$$\rho\left(\frac{\partial u}{\partial t}+u\frac{\partial u}{\partial x}+v\frac{\partial u}{\partial y}\right)=-\frac{\partial p}{\partial x}+\frac{\partial}{\partial x}\left\{\mu\left[2\frac{\partial u}{\partial x}-\frac{2}{3}\left(\frac{\partial u}{\partial x}+\frac{\partial v}{\partial y}\right)\right]\right\}+\frac{\partial}{\partial y}\left[\mu\left(\frac{\partial u}{\partial y}+\frac{\partial v}{\partial x}\right)\right]+X \tag{2}$$

$$\rho\left(\frac{\partial v}{\partial t}+u\frac{\partial v}{\partial x}+v\frac{\partial v}{\partial y}\right)=-\frac{\partial p}{\partial y}+\frac{\partial}{\partial x}\left\{\mu\left[2\frac{\partial v}{\partial y}-\frac{2}{3}\left(\frac{\partial u}{\partial x}+\frac{\partial v}{\partial y}\right)\right]\right\}+\frac{\partial}{\partial x}\left[\mu\left(\frac{\partial u}{\partial y}+\frac{\partial v}{\partial x}\right)\right]+Y \tag{3}$$

$$\rho c_p\left(\frac{\partial T}{\partial t}+u\frac{\partial T}{\partial x}+v\frac{\partial T}{\partial y}\right)=\frac{\partial}{\partial x}\left(k\frac{\partial T}{\partial x}\right)+\frac{\partial}{\partial y}\left(k\frac{\partial T}{\partial y}\right)+\mu\phi+\dot{q} \tag{4a}$$

$$\mu\phi=\mu\left\{\left(\frac{\partial u}{\partial y}+\frac{\partial v}{\partial x}\right)^2+\left[\left(\frac{\partial u}{\partial x}\right)^2+\left(\frac{\partial v}{\partial y}\right)^2\right]-\frac{2}{3}\left(\frac{\partial u}{\partial x}+\frac{\partial v}{\partial y}\right)^2\right\} \tag{4b}$$

Excluding viscous dissipation for the mixed convection flow regime and also there is no body force in the y-direction, eqn (3) becomes,

$$\left(\frac{\partial p}{\partial y}\right)=0 \tag{5}$$

Hence the x-pressure gradient at any point in the boundary layer must equal the pressure gradient in the quiescent region outside the boundary layer.

However, in this region (cylinder surface) u = v = 0 (no slip condition) so, eqn (2) becomes

$$\left(\frac{\partial p}{\partial x}\right)=-\rho_\infty g \tag{6}$$

Put eqn (6) in eqn (2), we have

$$u\frac{\partial u}{\partial x}+v\frac{\partial u}{\partial y}=\frac{g}{\rho}(\rho_\infty-\rho)+v\frac{\partial^2 u}{\partial y^2} \tag{7}$$

$$\text{Also, Let } \beta=-\frac{1}{\rho}\left(\frac{\partial \rho}{\partial T}\right)_\rho\approx-\frac{1}{\rho}\frac{\rho_\infty-\rho}{T_\infty-T} \tag{8}$$

It follows that$(\rho_\infty-\rho)\approx\rho\beta(T_\infty-T)$ put in

$$\frac{\partial u}{\partial t}+u\frac{\partial u}{\partial x}+v\frac{\partial u}{\partial y}=-\frac{1}{\rho}\frac{\partial p}{\partial x}+\ g\beta(T-T_\infty)+\ v\left(\frac{\partial^2 u}{\partial y^2}+\frac{\partial^2 u}{\partial x^2}\right) \tag{9}$$

So, the formulated governing equation becomes,

$$\frac{\partial u}{\partial x}+\frac{\partial v}{\partial y}=0 \tag{10}$$

$$\frac{\partial u}{\partial t}+u\frac{\partial u}{\partial x}+v\frac{\partial u}{\partial y}=-\frac{1}{\rho_\infty}\frac{\partial p}{\partial x}-g\beta(T-T_\infty)+\ v\left(\frac{\partial^2 u}{\partial y^2}+\frac{\partial^2 u}{\partial x^2}\right) \tag{11}$$

$$\frac{\partial v}{\partial t}+u\frac{\partial v}{\partial x}+v\frac{\partial v}{\partial y}=-\frac{1}{\rho_\infty}\frac{\partial p}{\partial y}+v\left(\frac{\partial^2 v}{\partial y^2}+\frac{\partial^2 v}{\partial x^2}\right) \tag{12}$$

For constant thermophysical properties, energy equation becomes;

$$\rho_\infty c_p\left(\frac{\partial T}{\partial t}+u\frac{\partial T}{\partial x}+v\frac{\partial T}{\partial y}\right)=k\left(\frac{\partial^2 T}{\partial y^2}+\frac{\partial^2 T}{\partial x^2}\right) \tag{13}$$

Free convection effects obviously depend on the expansion coefficient (β). The manner in which β is obtained depends on the fluid, for perfect gas,

Global Digital Central
ISSN: 2151-8629

$$\rho = \frac{P}{RT} \tag{14}$$

$$\text{So, } \beta = -\frac{1}{\rho}\left(\frac{\partial \rho}{\partial p}\right) = \frac{1}{\rho}\frac{P}{RT^2} = \frac{1}{T} \tag{15}$$

Where T is the absolute temperature for liquids and non-ideal gases, β must be obtained from appropriate property table.

Using the following relations to convert the governing equations to dimensionless form

$$x^* = \frac{x}{D},\quad t^* = \frac{D}{u_\infty},\ P^* = \frac{P}{\rho_\infty {u_\infty}^2}\ ,\ y^* = \frac{y}{D},\quad u^* = \frac{u}{u_\infty},\ v^* = \frac{v}{u_\infty},\ T^* = \frac{T-T_\infty}{T_s-T_\infty} \tag{16(a-g)}$$

The following are the dimensionless parameters used

$$Nu_D = \frac{hD}{k_\infty} = \frac{\partial T}{\partial n}|_{wall} \tag{17a}$$

$$C_D = \frac{2F_D}{\rho U_\infty^2 D} \tag{17b}$$

$$Pr = \frac{\mu C_p}{k} = \frac{\vartheta}{\alpha} \tag{17c}$$

$$Gr_D = \frac{g\beta(T_s - T_\infty)D}{u_\infty^2}\left(\frac{u_\infty D}{v}\right)^2 = \frac{g\beta(T_s - T_\infty)D^3}{v^2} \tag{17d}$$

$$\mathrm{R}e = \frac{\rho u \mathrm{D}}{\mu} \tag{17e}$$

Where k_∞ ($^W/_{m^2k}$) is the thermal conductivity of the fluid, h ($^W/_{m^2k}$) is the heat transfer coefficient, T is the dimensionless temperature, R n is the dimensionless coordinate normal to the cylinder F_D (N/m) is the drag force per unit length of the cylinder, ϑ ($^{m^2}/_S$) is the kinematic viscosity, α($^{m^2}/_S$) is the heat diffusivity.

$$D\partial x^* = \partial x, D\partial y^* = \partial y, u_\infty \partial u^* = \partial u,\ u_\infty \partial v^* = \partial v,\ (T_s - T_\infty)\partial T^* = \partial T \tag{18(a-e)}$$

Let

$$x^* = X,\ y^* = Y,\ u^* = U,\ v^* = V,\ T^* = T \tag{19(a-e)}$$

The governing equation in dimensionless form are,

$$\frac{\partial U}{\partial X} + \frac{\partial V}{\partial Y} = 0 \tag{20}$$

$$\left(\frac{\partial U}{\partial t} + U\frac{\partial U}{\partial X} + V\frac{\partial U}{\partial Y}\right) = -\frac{\partial P}{\partial X} + \frac{1}{Re}\left[\left(\frac{\partial^2 U}{\partial Y^2} + \frac{\partial^2 U}{\partial X^2}\right)\right] - \left(\frac{Gr}{Re^2}\theta\right) \tag{1}$$

$$\left(\frac{\partial V}{\partial t} + U\frac{\partial V}{\partial X} + V\frac{\partial V}{\partial Y}\right) = -\frac{\partial P}{\partial Y} + \frac{1}{Re}\left[\left(\frac{\partial^2 V}{\partial Y^2} + \frac{\partial^2 V}{\partial X^2}\right)\right] \tag{22}$$

$$\left(\frac{\partial \theta}{\partial t} + U\frac{\partial \theta}{\partial X} + V\frac{\partial \theta}{\partial Y}\right) = \frac{1}{Re.Pr}\left[\left(\frac{\partial^2 \theta}{\partial Y^2} + \frac{\partial^2 \theta}{\partial X^2}\right)\right] \tag{23}$$

Boundary Conditions

The boundary conditions used are;

a) Air inlet: u= U∞, T = T∞.
b) Air outlet: p = atmospheric pressure
c) The top and bottom surfaces fluid domain as well as the cylinder walls use the no slip wall boundary condition. Velocity at the walls V_w = 0
d) At a distance far away from the cylinder is at the free stream temperature T = T∞ and the cylinder walls is at constant temperature T=T_w

3. NUMERICAL SOLUTION

The software used for this work is ANSYS FLUENT 16.0 (FLUID FLOW). The solver uses finite element method, so it can handle complex geometry and complex boundary conditions efficiently. The software used for the statistical analysis is STATA/IC 12.0. The result obtained was also validated using MATLAB statistical tool. The inlet boundary condition was selected as *"velocity inlet"* for input of the airflow velocity. The velocity was varied from 0.81675 m/s to 0.081675 m/s for different formulation of Richardson number (Ri = Gr/Re) to be obtained. The Reynolds number 5591.362 (5.591e3) corresponding to the maximum velocity of 0.81675 m/s used is below the critical Reynolds number (2e5) for cylinder in cross flow so laminar condition is still maintained. The outlet uses the boundary condition of *"pressure-outlet" is set at default as gauge pressure of zero*. The profile walls are defined using the *"wall"* boundary condition; the side walls of the computational domain are defined as the *"symmetry"* boundary condition. Laminar viscous flow was assumed for the flow.

3.1. Statistical Test

Statistical test was conducted on the result to test the arrangements as groups or treatments. The test was to determine the arrangement that has the most, moderate and least significant influence on the heat transfer (Nusselt number) and coefficient of drag. The null hypothesis and alternative hypothesis are set as follow for both the transverse and longitudinal arrangement.
Where;

$$\mu_0\ reperesent\ the\ null\ hypothesis:$$
$$\mu_1\ represent\ the\ alternative\ hypothesis$$
$$S_{tn} represent\ the\ nth\ transverse\ arrangement$$
$$S_{ln} represent\ the\ nth\ longitudinal\ arrangement$$
$$\mu_0: S_{t1} = S_{t2} = S_{tn}$$
$$\mu_1: S_{t1} \neq S_{t2} \neq S_{tn}$$
$$\mu_0: S_{l1} = S_{l2} = S_{ln}$$
$$\mu_1: S_{l1} \neq S_{l2} \neq S_{ln}$$

If the calculated value is greater than the p-value (p-value= 0.05), the null hypothesis is accepted otherwise the null hypothesis is rejected and the alternative hypothesis is accepted. Also, interaction within the treatment is also obtained.

3.2. Model validation

This work was validated using correlation relation by Churchil and Berstein (Incropera and Dewitt, 1990) as shown in Table 1. Interestingly, there is a variation of 1.0235% between the present work and those of Churchil and Berstein (1995) values suggesting a close agreement.

Global Digital Central
ISSN: 2151-8629

Table 1 Validation of the present work with Churchill and Bernstein correlation

Nu	Churchill and Bernstein (incropera, 1995)	Present work	Error
Re = 100.02	5.178	5.231	1.0235%
Re = 5592.61	39.113	39.106	0.01826%

4. RESULTS AND DISCUSSION

4.1 Contour Plot of Pressure and Velocity Distributions

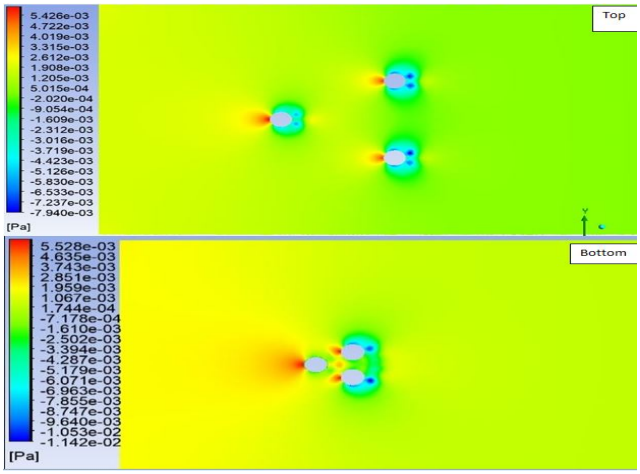

Fig. 1a Pressure contour at Ri =10, Pr=0.71. Top: SL/D=0.5, ST/D=0.5. Bottom: SL/D=0.15, ST/D=0.15

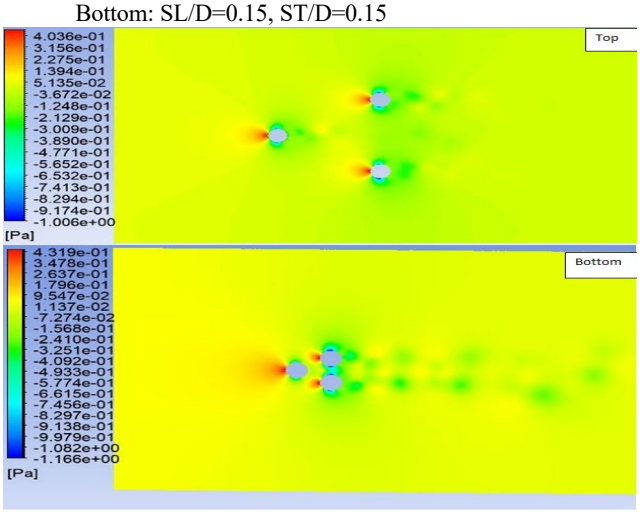

Fig. 1b Pressure contour at Ri =0.1, Pr=0.71. Top: SL/D=0.5, ST/D=0.5. Bottom: SL/D=0.15, ST/D=0.15.

The contour plot of pressure and velocity distributions are displayed for visualization of the flow behaviour as a function of cylinders' arrangement and Richardson number. Figures1a and 1b show the pressure contour within the flow domain. The pressure is at highest for all cases at the nose of the cylinders as indicated by the dense red colour because velocity is equal to zero at this point (stagnation point) and the pressure drops along the rear of the cylinders but with variation in intensity due to the effect of neighboring cylinders' arrangement and flow parameters. More precisely, Fig. 1a does not show any visible vortex shedding as compared to Fig. 1b, this is because Fig. 1b is an inertia dominated flow which have great influence on vortex shedding. Also, stagnation pressure is higher at Fig.1a bottom (low spacing) than Fig.1a top (high spacing), and thus result in high heat transfer rate. This is not surprising, it might likely due to low cylinders spacing interaction as shown in Fig. 1a bottom. Similarly, Fig.1b top and bottom show the same pattern but far higher stagnation pressure of order 100. This is due to the high kinetic head (high Reynolds number) which is converted to pressure head. Interestingly, Fig. 1b bottom shows higher vortex shedding than Fig. 1b top despite being at the same Ri. This reflects the effect of neighboring cylinders on the flow and thus suggests that cylinders' arrangement influence flow behaviour. Also, at higher cylinders spacing, the effect of cylinders' arrangement is negligible as shown in the two figures. Clearly, it is evident that cylinders arrangement has significant effect on the flow behaviour up to some certain value of cylinders' spacing where the cylinder does not have effect on one another.

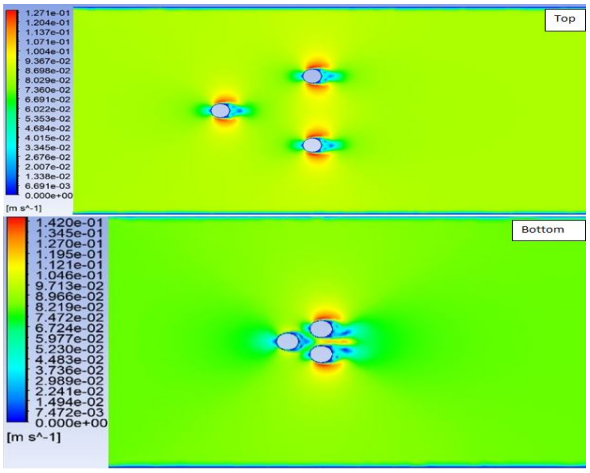

Fig. 2a Velocity contour at Ri =10, Pr=0.71. Top: SL/D=0.5, ST/D=0.5. Bottom: SL/D=0.15, ST/D=0.15.

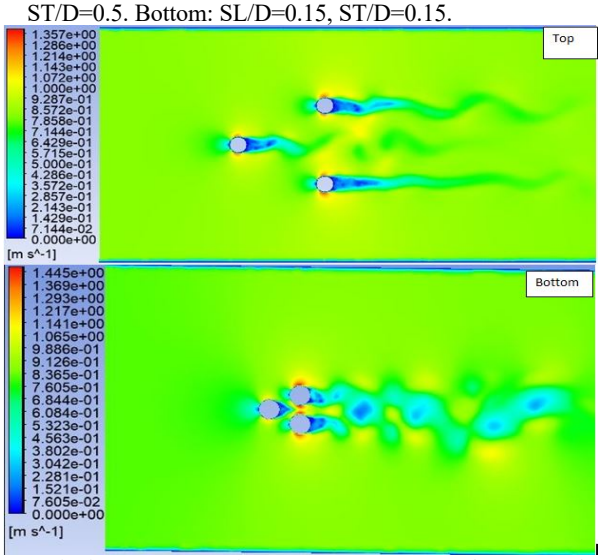

Fig. 2b Velocity contour at Ri =0.1, Pr=0.71. Top: SL/D=0.5, ST/D=0.5. Bottom: SL/D=0.15, ST/D=0.15.

Figures 2a and 2b shows the velocity contour within the flow domain. The velocity is at highest value at the top of the cylinders for all cases as indicated by the dense red colour because pressure is approximately equal to zero at that point but with different intensity due to the effect of cylinders' arrangement and flow parameters. More precisely, vortex shedding in Fig. 2b is highly pronounced than that of Fig. 2a. This is not surprising it is an indication of an inertia dominated flow which has great influence on vortex shedding. In addition, stagnation velocity is higher at Fig.2a bottom (low spacing) than Fig.2a top (high spacing), and thus will lead to low coefficient of drag. This

might suggest effect of low cylinders spacing interaction as shown in Fig. 2a bottom. Similarly, Fig.2b top and bottom show the same pattern. Further, as observed in pressure contour, Fig. 2b bottom shows higher vortex shedding than Fig. 2b top despite being at the same Ri. This corroborates the effect of neighboring cylinders on the flow as well as cylinders' arrangement influences on flow behavior. This effect reduces as the spacing increases as shown in the figures for SL/D=0.15, ST/D=0.15. Similar to Figures 1a and 1b, it can be inferred that cylinder's arrangement has significant effect on the flow behaviour up to some certain value of spacing. However, the effect reduces as the interaction between the cylinders is less pronounced.

4.2 Effect of cylinder arrangement on Nusselt number and Coefficient of drag for various Richardson numbers

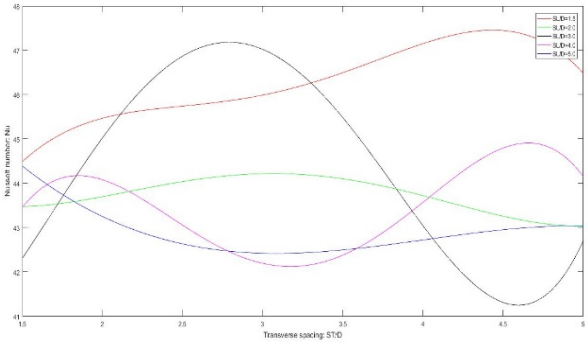

Fig. 3 Variation of Nusselt Number with Transverse Spacing at Ri = 0.1.

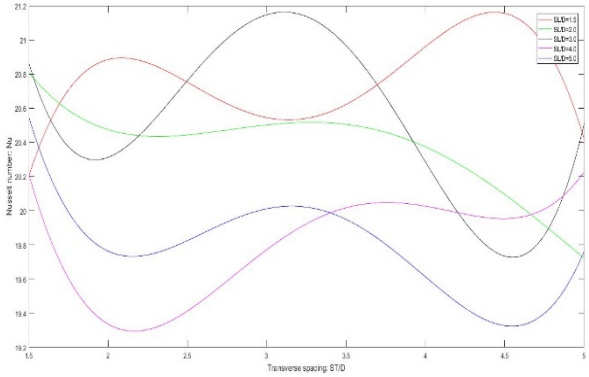

Fig. 4 Variation of Nusselt Number with Transverse Spacing at Ri=0.5.

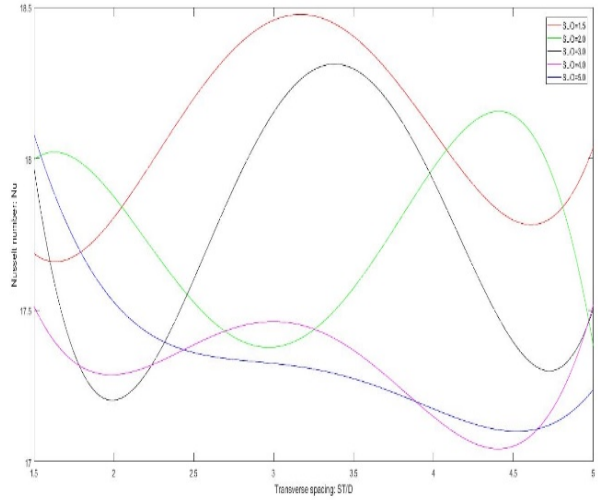

Fig. 5 Variation of Nusselt Number with Transverse Spacing at Ri=1.

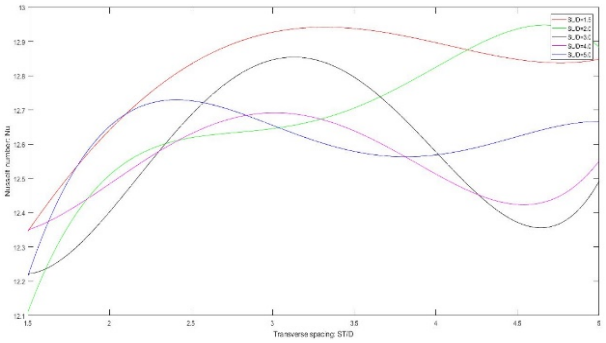

Fig. 6 Variation of Nusselt Number with Transverse Spacing at Ri=5.

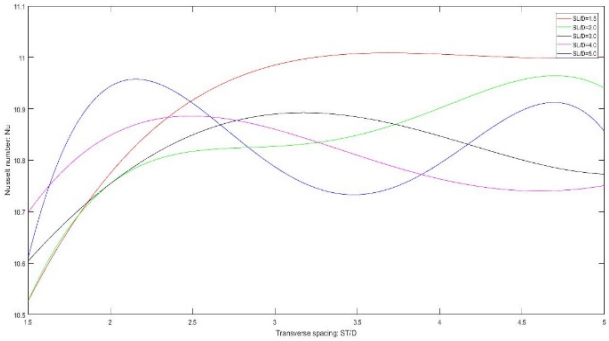

Fig. 7 Variation of Nusselt Number with Transverse Spacing at Ri=10.

The pressure and velocity contours showed that the interaction between cylinders are greatly influenced by spacing and Richardson number. The effect on Nusselt number and Coefficient of drag should sustanciate this influence as shown in Figures 3 to 16. The interesting thing in all the figures especially at lower spacing is that the magnitude and wavelength of oscillation of Nusselt number and Coefficient of drag is being controls by Richardson number Ri at least to some degree. For instance, Figures 3, 4, 5, 6and 7 show the variation of Nusselt number with transverse spacing for various SL/D at fixed Prandtl number Pr = 0.71 for Richardson number Ri = 0.1, 0.5. 1, 5 and 10, respectively.

From the figure, it can be seen that SL/D=1.5 have the highest Nu_Despecially at lower ST/D, suggesting that for inertia dominated flow the combination of low ratios of ST/D and SL/D might have the greatest effect on the Nu_D. This is not surprising since the effective region of pressure stagnation is minimal as a result of the effect of the neighboring cylinders and thus resulted in increase of stagnation velocity which eventually enhances the rate of heat transfer. Similarly, there is some disorderliness behaviours among the distributions suggesting a possible influence the cylinder arrangement can have on the behavior of Nu_D. This influence is control to some degree by the interaction of vortices among the cylinders as reflected in the velocity and pressure contours. The highest negative percentage difference of 9%, 7%, 5%, 2% and 2% as well as highest positive change of 7%, 4%, 6%, 4% and 3% for Ri = 0.1, 0.5. 1, 5 and 10, respectively were obtained within this arrangement indicating stepwise variation effect on the Nu_D. Therefore, the corresponding optimized arrangement for Nusselt number at Ri = 0.1, 0.5, 1, 5 and 10 were SL/D = 1.5 at ST/D = 4, SL/D = 3 at ST/D = 3, SL/D = 3 at ST/D = 3, SL/D = 3 at ST/D = 1.5, SL/D = 1.5 at ST/D = 4, respectively. It can be inferred that as Ri increases, the optimized arrangement also increases albeit marginally. It worth noting that some SL/D behave linearly to some degree within ST/D, suggesting that increasing spacing along the longitudinal direction does have linear effect on the heat transfer rate especially for SL/D that is within the influence of the flow field. The figures were replotted in figure 8 in order to understand the effect of Ri on flow dynamics taking into considerations the spacing arrangements. The Nusselt number of Ri = 0.1 is far higher than that of Ri=10, suggesting that inertia force has great

Global Digital Central
ISSN: 2151-8629

effect on heat transfer rate as compare to the buoyancy force. The effect decreases as Ri increases as observe in decrease in Nu_D.

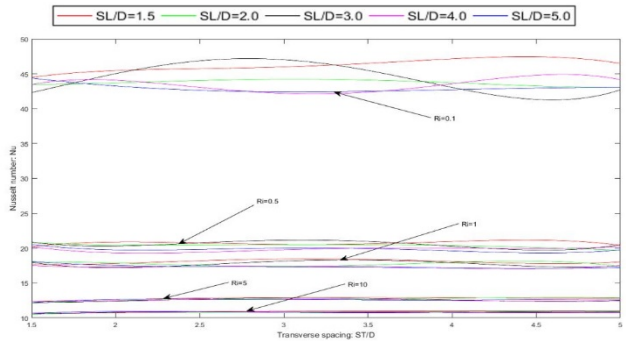

Fig. 8 Variation of Nusselt number with transverse spacing for various Ri.

The variation of coefficient of drag (Cd) with transverse spacing for various SL/D at Pr = 0.71 and Ri = 0.1, 0.5, 1, 5 and 10 were shown in figures 9, 10, 11, 12 and 13, respectively. The significant effect of spacing on Cd is clearly evidenced in all the spacing arrangements. While the magnitude is altered as Ri changes, it seems that the wavelength and oscillation is barely unaltered. This might suggest that Ri might not give a true representation of the interaction of the cylinders in the field. This is consistent with the observations of the wake formation and vortex shedding. The randomness observed in the figure might be due to the vortices formed as a result of the arrangement which in turn has great effect on the Cd. Similar to NuD, the highest negative percentage difference of 34%, 16%, 19%, 7% and 8% as well as highest positive change of 39%, 16%, 11%. 15% and 10%for Ri = 0.1, 0.5. 1, 5 and 10, respectively were obtained based on pointwise variation on the Cd. This shows the effect of arrangement on the Cd from one arrangement to another.

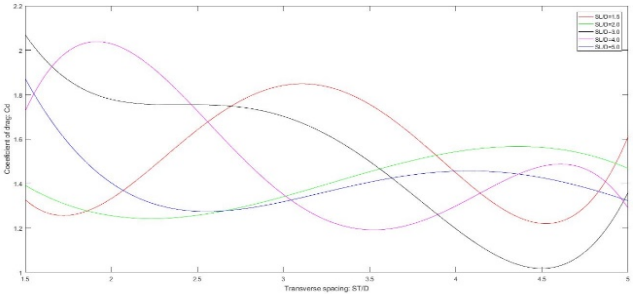

Fig. 9 Variation of Coefficient of Drag with Transverse Spacing at Ri = 0.1.

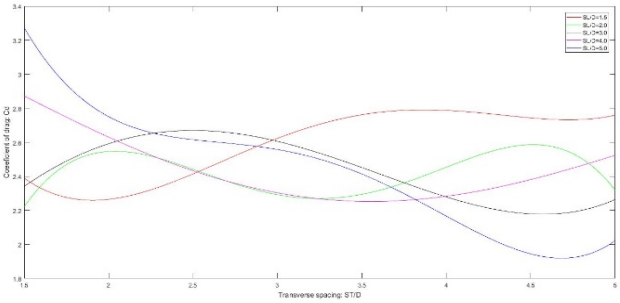

Fig. 10 Variation of Coefficient of Drag with Transverse Spacing at Ri=0.5.

Figure 14 shows the variation of coefficient of drag with transverse spacing at Ri =0.1, 1, 10. The previous figures were replotted to the Ri influence of Cd. The Ri=0.1 plot is the most disorganized which is due to the high effect of Reynolds number (inertia effect) over Grashof number (buoyancy effect) compare especially to Ri=10. The chaos decreases with increase in Ri significantly. This imply that despite being within the same zone (mixed convective zone) classification, the behaviour varies significantly and thus, details tight zone (the Reynolds number, Grashof number and other variables must be clearly stated) analysis will be the best generalization.

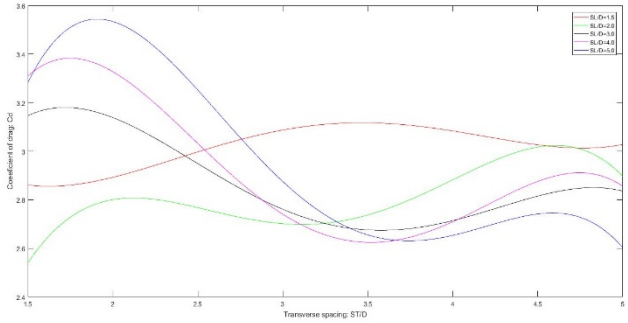

Fig. 11 Variation of Coefficient of Drag with Transverse Spacing at Ri =1.

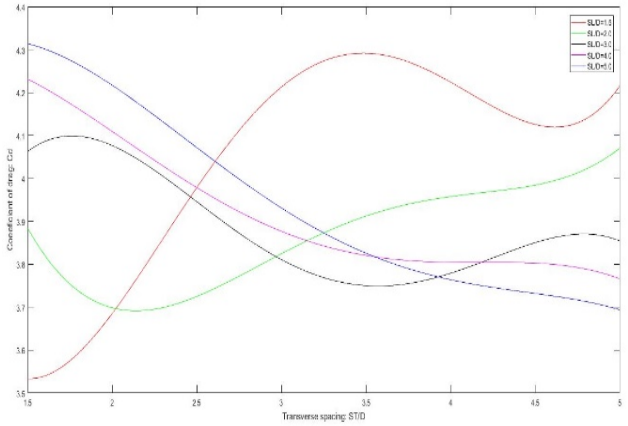

Fig. 12 Variation of Coefficient of Drag with Transverse Spacing at Ri =5.

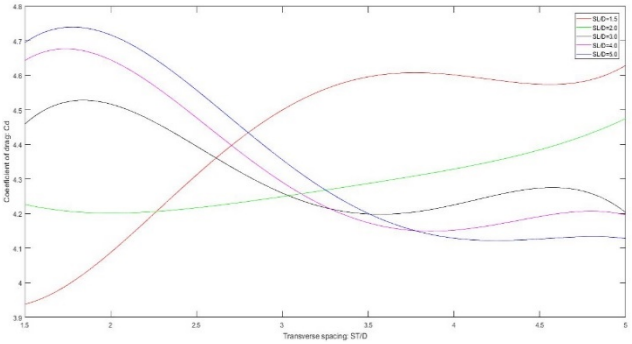

Fig. 13 Variation of Coefficient of Drag with Transverse Spacing at Ri =10.

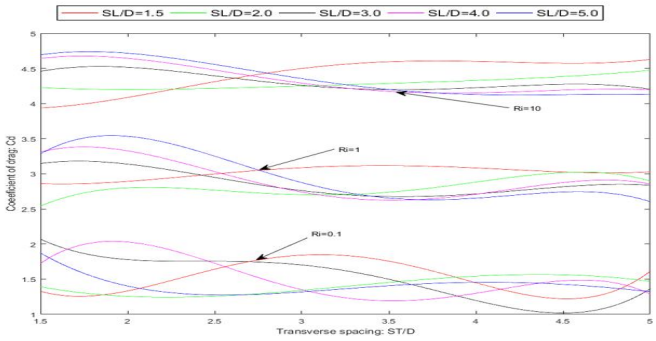

Fig. 14 Variation of coefficient of drag with transverse spacing for Ri= 0.1, 1 and 10.

In order to further ascertain the changes that occur in the field as a result of the interaction among the cylinders, Figures 15 and 16 show the effect of cylinders arrangement on NuD and Cd at two different values of Ri=0.1 and 10 being the two special cases of inertial (Ri=0.1 implies effect of Re> effect of Gr) and bouyancy ((Ri= 10 implies effect of Gr> effect of Re) dominated flow.

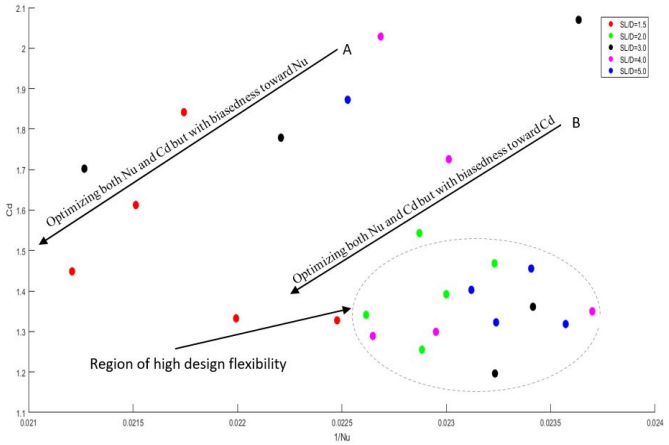

Fig. 15 Variation of Inverse of Nusselt Number with Coefficient of Drag at Ri=0.1.

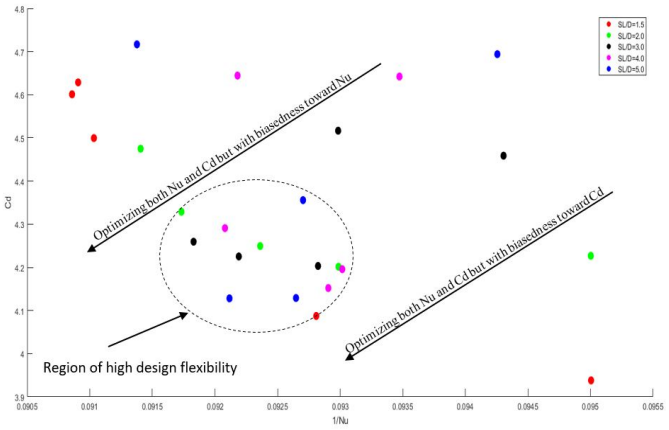

Fig. 16 Variation of Inverse of Nusselt Number with Coefficient of Drag at Ri =10.

Figures 15 and 16 shows the multivariate behaviour of the system as compare to figures 9 and 13 which only show the univariate behaviour of Cd alone without taking Nu into consideration under the effect of experimental variables (ST/D, SL/D and Ri). The figure is necessary in order to visualize the objectives variation so as to obtain an optimized system taking both Cd and Nu_D into consideration. The highly randomness of figure 15 is due to great dominance of inertia force as a result of the high Reynolds number. The implication of this is that it will lead to decrease in the drag coefficient on the cylinder surface due to high rate of vortices detachment. Line A shows the direction of optimization of both Nu and Cd but with more biasedness toward Nu, moving along the direction of line A, the more the system is optimized although the optimization of Nu is more prioritized than that of Cd. Similarly, Line B shows the direction of optimization of both Nu and Cd but with more biased toward Cd, moving along the direction of line B, the more the system is optimized although the optimization of Cd is more prioritized than that of Nu. The encircled region in the figure is the region with high design flexibility because it has more design points than other regions. Drawing a line from the 1/Nu and/or Cd axes marking a desire value of 1/Nu and/or Cd will produce many alternative/designs within this encircled region. This region corresponds with low Nu, low Cd at smaller spacing of SL/D with different spacing of ST/D. This shows that ST/D (transverse spacing) does not have significant effect on Cd and Nu at smaller spacing of SL/D. Moreover, the relatively orderliness of figure 16 as compared with figure 15 is due to low dominance of inertia force as a result of the low Reynolds number. This eventually leads to high drag coefficient on the cylinder surface due to low rate of vortices detachment. This is not surprising, since at low Reynolds numbers, it was evidenced that some symmetrically placed vortices downstream of the cylinder about the channel centerline, remain attached to the cylinder. The top line shows the direction of optimization of both Nu and Cd but with more biased toward Nu. Moving along the direction of line A, the more the system is optimized although the optimization of Nu is more prioritized than that of Cd. Bottom line shows the direction of optimization of both Nu and Cd but with more biased toward Cd. It should be noted that moving along the direction of line B, the more the system is optimized taking into consideration that the optimization of Cd is more prioritized than that of Nu. Besides, the centre line between top line and bottom line shows a condition where the Cd and Nu are prioritized equally. The encircled region in the figure is the region with high design flexibility because it has more design points than other regions. Drawing a line from the 1/Nu and/or Cd axes marking a desire value of 1/Nu and/or Cd will produce many alternatives /designs within this encircled region.

5. CONCLUSIONS

In this present work, numerical investigation of mixed convective heat transfer over triangular arranged cylinders for varying Reynolds numbers were conducted. The main objective of this work was to obtain optimized arrangement for a mixed convective heat transfer over triangularly arranged cylinders through the maximization of Nusselt number and minimization of drag coefficient. Reynolds number was varied, while the Grashof number was kept constant for mixed convective regimes formulation (Richardson numbers Ri=0.1 to 10) to be obtained. The Reynolds number 5591.362 (5.591e3) corresponding to the maximum velocity of 0.81675m/s used, is below the critical Reynolds (2e5) for cylinder in cross flow so laminar condition is still maintained. The geometric arrangement selection SL/D= 1.5, 2, 3, 4 and 5 and ST/D=1.5, 2, 3, 4 and 5 were used for this study. Statistical tools were also used to determine significant effect of the spacing on the Nusselt number and coefficient of drag. The boundary was insulated to avoid heat gain or loss to the surrounding. The model governing equation was solved using finite element technique with the aid of ANSYS fluent software. The mean of the Nusselt number and drag coefficient over the three cylinders were evaluated. The results were also analyzed statistically to determine how significant are the effect of the variables. The study showed an optimized arrangement of 50% difference in coefficient of drag and 10% difference in Nusselt number within geometrical arrangement variation. Also, the results showed that flow regimes have effect on the heat transfer and drag coefficient. The conclusions that can be drawn from this computational study are summarised as follows:

i) Ri=0.1 has the highest variation due to the significant effect of inertia force over buoyancy force, while Ri=10 has the least variation due to the significant effect of buoyancy force over inertia force.
ii) It is not sufficient to generalize the behaviour of heat and fluid flow by varying one parameter (i.e. Reynold number) and keeping others (i.e. Grashof number) constant within a global classification. This work showed that variation of one of the variables of dimensionless number is not sufficient to justify the other variables due to local flow regimes.
iii) At large spacing, where there is little effect of neighboring cylinders, the Nusselt numbers and coefficient of drag were almost the same with flow condition as if there were no other cylinders.
iv) The study showed that Cd and Nu are highly sensitive to flow regimes as well as the geometric arrangement so analysis will be required for all system to be designed.

v) The work showed that the regimes of hydrodynamics and thermal fields determined the optimized arrangement for triangularly arranged cylinders as a result of varying behaviour at different flow parameters. Furthermore, the statistical analysis showed that variation of Cd is not so significant compared to the variation of Nu.

REFERENCES

Abed, I.M., Ali, F.H. and Sahib, S.A.M 2020, *"Investigation of Heat Transfer and Fluid Flow around Sinsoudal Corrugated Circular Cylinder for Two Dimensional System",* Frontiers in Heat and Mass Transfer (FHMT), 15: 6. https://doi.org/10.5098/hmt.15.6

Alansar, H., Zeitoun, O. and Ali, M. 2012, *"Numerical Modeling of Natural Convection Heat Transfer around Horizontal Triangular Cylinders",* Journal of Numerical Heat Transfer, Part A 61: 201–219. https://doi.org/10.1080/10407782.2011.643734.

Ali, M.H. and Jalal, R.E., 2020, *"Natural Convection in a Square Enclosure with Different Openings and Involves Two Cylinders: A Numerical Approach",* Frontiers in Heat and Mass Transfer (FHMT), 15: 27. https://doi.org/10.5098/hmt.15.27.

Alinejad, J. 2016, *"Lattice Boltzmann Simulation of a Fluid Flow around a Triangular Unit of Three Isothermal Cylinders",* Journal of Applied Mechanics and Technical Physics, 57(1): 117-126. https://doi.org/10.1134/S0021894416010132.

Amir F.M.,Yusoff, M.Z. and Hassan, S.H.A., 2022, *"Characteristics and Thermal Performance of Nanofluid Film over Horizontal Multi-Faceted Cylinder"*, Frontiers in Heat and Mass Transfer (FHMT), 18: 27. https://doi.org/10.5098/hmt.18.27.

Barros, G. M., Lorenzini, G.L.A.,Isoldi, L. A. , Rocha, L. A. O. and Dos Santos, E.D., 2017, *"Influence of Mixed Convection Laminar Flows on The Geometrical",* International Journal of Heat and Mass Transfer, 13: 234-415.
https://doi.org/10.1016/j.ijheatmasstransfer.2017.07.010.

Bello-Ochende, T. and Bejan, A., 2004, *"Optimal Spacing for Mixed Convection",* Journal of Heat Transfer, 126(6): 956-962. https://doi.org/10.1115/1.1833363.

Elazm, M.M.A., Shahata, A.I., Elsafty, A.F. and Teamah. M.A., 2015, "*Numerical Investigation of a Three-Dimensional Laminar Mixed Convection Flows in Lid-Driven Cavity for very Small Richardson Number"*, Proceedings of the ASME 2015 Power Conference, San Diego, California.
https://doi.org/10.1115/POWER2015-49575.

Gu, Z. F. and Sun, T., 1999, *"On Interference of Two Circular Cylinders in Staggered Arrangement at High Subcritical Reynolds Number",* Journal of Wind Engineering. Industrial Aerodynamics, 80: 287-309. https://doi.org/10.1016/S0167-6105(98)00205-0.

Hu, H. and Koochesfahani, M.M., 2005, *"The Wake Behavior behind a Heated Cylinder in Forced and Mixed Convection Regimes",* Proceedings of HT05 Westin St. Francis, San Francisco, CA, USA. https://doi.org/10.1115/HT2005-72766.

Incropera, F.P., and Dewitt, D.P., 1990, Introduction to heat and mass transfer. 2nd ed. Pg. 381 Singapore: John Wiley and Sons.

Johansson, S.H., Davidson, L. and Olsson, E. 1993, *"Numerical Simulation of Vortex Shedding Past Triangular Cylinders at High Reynolds Number using a K-8 Turbulence Model",* International Journal for Numerical Methods in Fluids, 16: 859-878. https://doi.org/10.1002/fld.1650161002.

Lam, K. and Cheung, W.C., 1988, *"Phenomena of Vortex Shedding and Flow Interference of three Cylinders in Different Equilateral Arrangements"*, Journal of Fluid Mechanics, 196: 1–26. https://doi.org/10.1017/S0022112088002587.

Ohya, Y., Okajima, A. and Hayashi, M., 1989, Wake interference and vortex shedding, in: N.P. Cheremisinoff (Ed.), in collaboration with G. Akay, Encyclopedia of Fluid Mechanics, Gulf Publishing, Houston.

Osborne, D.G. and Incropera, F.P., 1985, Heat and mass transfer. John Wiley & Son.

Price, S.J., Paidoussis, M.P. and Mark, B., 1995, *"Flow Visualization of the Interstitial Cross-Flow Through Parallel Triangular and Rotated Square Arrays of Cylinders",* Journal of Sound and Vibration, 181(1): 85-98.
https://doi.org/10.1006/jsvi.1995.0127.

Sahu, K. B. and Singh, R. K., 2014, *"Analysis of Heat Transfer and Flow due to Natural Convection in Air around Heated Triangular Cylinders of Different Sizes Inside a Square Enclosure"*, Journal of Heat and Mass Transfer, 21: 234-246.
https://doi.org/10.1016/j.proeng.2014.11.771.

Wang, C.Y., 1998, "Longitudinal Flow Past Cylinders Arranged in a Triangular Array", Elsevier Inc. https://doi.org/10.1016/S0307-904X(98)10075-6.

Wang, Z., Wang, Z. and Yang, M., 2021, *"Transversal Flow and Heat Transfer of Two Cylinders with a Flapping Reed between them",* Frontiers in Heat and Mass Transfer (FHMT), 17, 10. https://doi.org/10.5098/hmt.17.10.

Zdraovich, M.M., 1977, *"Review of Flow Interference between two Circular Cylinders in Various Arrangements"*, Journal of Fluids Engineering, 99(4): 618–633.
https://doi.org/10.1115/1.3448871.